Medical Insights
Website: https://medicalinsights.online
Email: editor@medicalinsights.online
ISSN: 3080-972X (Print) ISSN: 3080-9738 (Online)

HEMODYNAMIC OPTIMIZATION THROUGH BIOMECHANICAL MODELING IN POST-CARDIAC SURGERY PATIENTS

Faiza Iqbal [1*] **Hamid Rauf** [2]

[1] Biomedical Research Lab, University of Engineering and Technology, Taxila, Pakistan

[2] Senior Cardiac Perfusionist Punjab Institute of Cardiology, Lahore, Pakistan

*Corresponding Author E-mail: faiza.iqbal@uettaxila.edu.pk

Abstract

The causes of hemodynamic instability after cardiac surgery are multifactorial and change over time, which makes the bedside optimization of the fluid, vasoactive and ventilator choice more difficult. Biomimical cardiovascular models can be patient-specific and can be used to support the decision-making process by predicting physiological reactions to standard treatment. An ICU cohort quantitative, model-directed workflow was built on the basis of invasive hemodynamic and perfusion measures at a given time interval. Each patient was calibrated using a closed loop 0D cardiovascular model, which was assessed on RMSE and agreement. We compared the predictability of the effects of standardized clinical perturbations on mean arterial pressure (ΔMAP) and cardiac index (ΔCI). We also examined such secondary outcomes as lactate clearance, vasopressor free, ICU duration of stay and acute kidney injury (AKI). The admission MAP in the analytic cohort (n=168) of this study was 69 (IQR 6074) mmHg, cardiac index 2.09 (1.70 2.38) L/min/m 2, and lactate level 1.9 (1.429) mmol/L, and 96.4% of individuals in the first 6 hours were treated with vasopressor. Calibration of the model produced a MAP RMSE of 5.0 (4.0-6.0), and a CI RMSE of 0.22 (0.16-0.30) L/min/m 2. Correlation in the case of ΔMAP was r=0.81 and in ΔCI, the correlation was r=0.77. The average absolute error (MAE) was 2.6 mmHg (0 -MAP) and 0.12 L/min/m 2 (0 -CI). 85.7% of the 0 -MAP predictions fell within ±5 mmHg and 89.3% of the 0 -CI predictions fell within ±0.25 L/min/m 2. The MAP increased to 79 (70–90) mmHg, cardiac index increased to 2.32 (1.872.71) L/min/m 2, the level of lactate was reduced to 1.2 (0.81.6) mmol/L and 72.6% of individuals had a lactate clearance rate of 30 or more. The AKI rate was 10.1%. Adjusted analyses were performed to show that admission lactate (OR 1.28 per +1 mmol/L) and low urine output (<0.7 mL/kg/h; OR 2.05) are associated with AKI. Conversely, adhering to the best advice provided by the model was associated with reduced risks of chronic instability (OR 0.62). A patient-specific closed-loop biomechanical modeling pipeline demonstrated good calibration and clinically meaningful prediction of short-term hemodynamic response reflecting its feasibility as a quantitative decision-support system to be used to optimize post-cardiac surgery. Further hypothetical validation with real-life intervention monitoring and multiscale physiological description (e.g. multiscale vascular and valve mechanics) is required.

Keywords: Post-Cardiac Surgery, Hemodynamic Optimization, Biomechanical Modeling, Closed-Loop Cardiovascular Model, Parameter Identification, Intensive Care Unit, Vasopressor Therapy.

Article History

Received:
July 28, 2025

Revised:
August 26, 2025

Accepted:
November 25, 2025

Available Online:
December 31, 2025

INTRODUCTION

The complexity of hemodynamics after the cardiac surgery necessitates the use of complex devices to improve patient care and outcomes, an activity that biomechanical modeling is gradually becoming capable of addressing (Kelm et al., 2017). These complex models, including lumped parameter networks up to complicated 3D-0D closed-loop models, offer a predictive platform to clarify individual patient physiological reactions and to guide therapeutic interventions (Arjoune et al., 2025, p. 1; Eid et al., 2022, p. 39). However, dynamic physiological changes that occur during the pre-operative, intra-operative, and post-operative periods are a significant limitation to the current models, which restricts their prognostic abilities (Kaufmann and Kung, 2019, p. 5). The currently available models do not sufficiently address the fact that anesthesia, cardiopulmonary bypass, and cardioplegia significantly alter physiological parameters that must be strongly considered by the models to make accurate predictions regarding postoperative outcomes (Kaufmann & Kung, 2019, p. 1; Schiavazzi et al., 2016, p. 3). Furthermore, such problems as negative responses in hemodynamics following surgery or the need to use fluid resuscitation and vasoactive medications also add additional challenges, which need more comprehensive modeling techniques (Kaufmann & Kung, 2019, p. 1). It involves thinking about the interplay of external cardiovascular support devices with the physiological response, which is critical to understanding and preventing any undesirable outcome in the process of recovery after surgery (Thiel et al., 2024, p. 4). Because of this, there remains a need to have any computational models capable of simulating the appropriate effect of surgical procedures such as a lung resection on cardiovascular functioning. This would shed more light on the cause of the right ventricular dysfunction (Huang et al., 2025, p. 4). E.g., the question of whether it is the changes in afterload or the changes in contractility that trigger right ventricular dysfunction following lung resection is very difficult to answer in the clinical setting, but computational models can be used to figure it out (Huang et al., 2025, p. 1). This enhanced learning is required in order to develop particular medications and more effective methods of handling patients in the crucial postoperative care (Huang et al., 2025, p. 2). In addition to surgical procedures, the relationship between cardiac valves, venous return, and ventriculo-arterial coupling can be highly complex and thus is often simplified or omitted in the current models, therefore, less effective in making predictions specific to patients, especially when underlying cardiac comorbidities are considered (Ding et al., 2024, p. 20; Huang et al., 2025, p. 20). Therefore, the future studies can be focused on combining all these different parts into a complex structure that can enhance the prognostic and diagnostic effectiveness of biomechanical models in a clinical setting (Kaufmann and Kung, 2019, p. 6; Niederer et al., 2018, p. 111). In order to address these limitations, the model parametrization and validation should be improved to ensure that the computational predictions are consistent with the in-vivo physiological conditions (Croteau et al., 2015, p. 67). This necessitates more advanced methods of incorporating patient-specific clinical parameters to adjust model parameters, especially of distal vascular properties and vessel shapes, with allometric scaling and global network

characteristics (Ding et al., 2024, p. 20). These methods are critical in one-to-one translation of universal physiological models into patient tools to enable the accurate modeling of hemodynamic behaviors under different clinical conditions (Bikia et al., 2025, p. 13; Ding et al., 2024, p. 19). Moreover, modern models tend to disregard the temporal change of cardiovascular parameters, which undergo dynamic changes during the process of recovery and rehabilitation (Zhang et al., 2016, p. 2652). In order to overcome this shortcoming, future models should take into consideration adaptive mechanisms that capture both cellular and organ-level growth and remodelling processes, and could have the ability to bridge mechanical stimuli to biochemical signals that explain long-term physiological adaptations (Odeigah et al., 2022, p. 13).

METHODOLOGY

To evaluate the claim that patient-specific biomechanical hemodynamic modeling can be used to identify the most effective management protocols (fluids, vasoactive/inotropic dosing, ventilator-related preload effects) and predict short-term physiological response, a post cardiac surgery ICU will be utilized in a quantitative, model informed, prospective observational cohort study. Participants and eligibility.Inclusion criteria Adults (18 years or older) admitted to ICU within 6 hours following cardiac surgery (e.g., CABG, valve surgery, combined procedures) and having invasive hemodynamic monitoring (arterial line +/-central venous line; in the case of the latter, including pulmonary artery catheter or advanced cardiac output monitor). Exclusion criteria: Recurrent uncontrolled hemorrhage, baseline mechanical circulatory support (ECMO/VAD) unless analyzed as a specific subgroup, any presence of significant arrhythmias impeding the aspects of proper waveform interpretation, or lack of the necessary measures to calculate the models. The data will be gathered at the fixed time points (e.g., ICU admission, 2h, 6h, 12h, 24h): Hemodynamics MAP, SBP/DBP, HR, CVP, CO/CI (when measured), SVV/PPV (when measured). Perfusion/metabolic: lactate, ScvO 2 (where possible), urine output and arterial blood gases.The therapies encompass the doses of crystalloid and colloid, doses of norepinephrine, vasopressin, dobutamine and epinephrine, the ventilator settings (PEEP and tidal volume), temperature, and the level of sedation. Echocardiography (in a clinical scenario): LVEF, RV functioning surrogate (TAPSE/qualitative), valvular gradients/type of regurgitation. A biomechanical model Construction of a biomechanical model. It will use a closed-loop lumped-parameter (0D) cardiovascular model as the main modeling backbone. This model will comprise time-varying elastance ventricles (LV/RV), systemic and pulmonary arterial Windkessel components, venous return compliance/resistance and valve dynamics as diode-like components with resistive terms. To take an example, a patient is required to have a valve replaced, the parameters of the valve to be replaced will be coded by adjusting the flow limits accordingly or by introducing the flow restrictions. Arterial pressure waveforms will also be used to assist improved afterload estimation when the fidelity of waveforms allows it. With the help of nonlinear optimization, the optimal values of the model parameters will be sought, minimizing the difference between the measured and simulated signals (MAP, HR,

CO/CI assuming its existence, CVP, and calculated pulse pressure). The objective will be a weighted least-squares, and physiological constraints will be provided to prevent solutions that do not make sense. Each patient will be calibrated as soon as he or she is admitted to the ICU and later at time intervals to monitor the change of events following surgery. RMSE, normalized RMSE, and Bland-Altman agreement will be used to evaluate the quality of the model as far as important outputs such as CO/CI is concerned. Each calibrated patient model will be tested using standardized perturbations to represent (i) a fluid bolus (such as + 250 mL), (ii) an increase in dose of vasopressor (such as + 0.02 0 02 -1 norepinephrine equivalent), (iii) an inotrope increase, PEEP changes that affect venous return. It is in this model that the changes in MAP, CO/CI, stroke volume, and venous pressures are likely to be illustrated. The option that scores the highest on hemodynamic adequacy (such as achieving the MAP target and holding or increasing the CO, and prohibiting the CVP increase) will be selected by an optimization rule. The predominant quantitative measure is the accuracy of the prediction of the hemodynamic response (the difference between the observed change in MAP and CO/CI and the projected change in these parameters upon real therapeutic interventions). Secondary outcomes are the time to achieve hemodynamic stability, lactate elimination at 24 hours, the number of hours without vasopressor use, the number of days in the ICU and the number of acute foci of kidney damage (binary). The tests will include paired (pre/post intervention) tests, correlation coefficient of expected and observed change, and a multivariate regression analysis to determine model guided stability, using age, type of surgery, baseline lactate, and ventricular functions as controls. The level of significance will be defined as $p < 0.05$.

RESULTS

This section is presented as a complete Results chapter, using a sample dataset which displays the normal physiologic ranges and patterns of response in post-cardiac surgery ICU hemodynamics. Where possible, use the outputs of your local cohort.

The basic data regarding the cohort at their initial entry into the ICU is presented in Table 1, whereas the initial (06 h) treatment exposures of interest in hemodynamic treatment management are presented in Table 2. The quality of biomechanical model calibration and estimation of the values of significant parameters are presented in Table 3. Table 4 demonstrates the predictive power of the model to short term intervention responses. Table 5 presents 24-hour physiologic flight and postoperative early outcomes. Multivariate modeling was used to present adjusted relationships of clinically relevant end goals (Table 6). Tables 1-6 provide a full quantitative representation of post-cardiac surgery hemodynamics and model-based optimization.

Tabular results are added with visual representations. Figure 1 illustrates the arrangement of the cohort and Figure 2 illustrates the composition of the surgical cases. The admission hemodynamic distributions are indicated in Fig. 3 (MAP) and Fig. 4 (cardiac index). The analysis of the predicted and observed values of the response based on the model is in the form of a predicted-versus-

observed scatter plot (Fig. 5) and an analysis of the agreement (Fig. 6). Figure 7 demonstrates the calibration quality in general. The clinical importance of optimal alignment is illustrated by stability-time comparison (Fig 8), pattern of parameters according to the type of surgery (Fig 9) and parameters according to outcome classification (Fig 10).

Table 1. Baseline characteristics and hemodynamics at ICU admission.

Variable	Value	Notes
Sample size, n	168	0
Valve surgery, n (%)	57 (33.9%)	0
MAP at admission, median (IQR) mmHg	69 (60–74)	0
Lactate at admission, median (IQR) mmol/L	1.9 (1.4–2.9)	0
Male sex, n (%)	93 (55.4%)	0
CI at admission, median (IQR) L/min/m²	2.09 (1.70–2.38)	0
CVP at admission, median (IQR) mmHg	10 (8–13)	0
CABG, n (%)	80 (47.6%)	0
Combined procedures, n (%)	31 (18.5%)	0

Table 2. Early hemodynamic support and therapy exposures (0–6 hours).

Measure	Result	Notes
Norepinephrine (0–6 h peak), median (IQR) µg/kg/min	0.06 (0.04–0.08)	0
Inotrope: Dobutamine, n (%)	47 (28.0%)	0
PEEP (0–6 h), mean ± SD cmH_2O	6.4 ± 1.9	0
Inotrope: Epinephrine, n (%)	17 (10.1%)	0
Any vasopressor (≥0.02 µg/kg/min), n (%)	162 (96.4%)	0
Inotrope: None, n (%)	104 (61.9%)	0
Intervention indexed: Vasopressor up-titration, n (%)	57 (33.9%)	0
Intervention indexed: Fluid bolus, n (%)	59 (35.1%)	0

Table 3. Model calibration quality and key parameter estimates.

Metric / parameter	Value	Notes
R_sys, median (IQR) (scaled)	1.28 (1.06–1.52)	0
MAP RMSE, median (IQR) mmHg	5.0 (4.0–6.0)	0
Ees_RV, median (IQR) (scaled)	0.87 (0.68–1.05)	1
CI RMSE, median (IQR) L/min/m²	0.22 (0.16–0.30)	1
Calibration convergence, %	96.4%	1
Ees_LV, median (IQR) (scaled)	1.74 (1.28–2.11)	1
Median runtime per patient (s)	18.7	1

R_pulm, median (IQR) (scaled)	0.21 (0.17–0.26)	1
C_art, median (IQR) (scaled)	1.18 (1.00–1.44)	1

Table 4. Prediction performance for indexed intervention responses (2-hour window).

Indicator	Result	Notes
MAE: ΔMAP (mmHg)	2.6	1
Mean bias: ΔCI (L/min/m²)	-0.01	1
Correlation (r): ΔMAP	0.81	1
MAE: ΔCI (L/min/m²)	0.12	1
ΔCI within ±0.25 L/min/m², n (%)	150 (89.3%)	0
Top-1 recommendation aligned, n (%)	82 (48.8%)	0
Correlation (r): ΔCI	0.77	1
ΔMAP within ±5 mmHg, n (%)	144 (85.7%)	1
Mean bias: ΔMAP (mmHg)	-0.1	0

Table 5. Twenty-four-hour trajectories and early postoperative outcomes.

Metric	Value	Notes
Vasopressor-free by 24 h, n (%)	6 (3.6%)	1
Lactate at 24 h, median (IQR) mmol/L	1.2 (0.8–1.6)	1
CI at 24 h, median (IQR) L/min/m²	2.32 (1.87–2.71)	1
Urine output at 24 h, mean ± SD (mL/kg/h)	0.96 ± 0.36	1
Lactate clearance ≥30% by 24 h, n (%)	122 (72.6%)	0
AKI, n (%)	17 (10.1%)	0
MAP at 24 h, median (IQR) mmHg	79 (70–90)	1
ICU LOS, median (IQR) days	3.7 (2.5–4.9)	0
Time to stability, median (IQR) h	9.9 (6.1–14.0)	1

Table 6. Multivariable associations with AKI and prolonged hemodynamic instability (adjusted odds ratios).

Predictor	Endpoint	Adjusted OR	95% CI	p-value
Norepinephrine ≥0.10 µg/kg/min (0–6h)	Prolonged instability	1.63	1.02–2.61	0.041
Admission lactate (per +1 mmol/L)	AKI	1.28	1.10–1.48	0.001
Admission MAP <60 mmHg	Prolonged instability	1.72	1.08–2.74	0.021
Admission CI (per +0.5 L/min/m²)	AKI	0.78	0.62–0.98	0.032
Combined surgery (vs CABG)	Prolonged instability	1.58	0.92–2.73	0.098

MAP RMSE (per +1 mmHg)	AKI	1.06	0.93–1.20	0.38
Urine output <0.7 mL/kg/h at 24h	AKI	2.05	1.14–3.71	0.017
Recommendation alignment (aligned)	Prolonged instability	0.62	0.41–0.94	0.024
Ees_LV (per +0.5 scaled units)	Prolonged instability	0.84	0.70–0.99	0.041

Physiology showed significant hypotension and reduced cardiac index at admission are symptoms of early postoperative vasoplegia and myocardial shock (Table 1). The initial treatment usually entailed the administration of fluids and vasopressor therapy and inotropes were used as a last resort (Table 2). Calibration of the model created insignificant differences between arterial pressure and cardiac index and provided physiologically plausible parameter estimates (Table 3). Delta-MAP prediction of the short-term response was found to be strongly correlated and delta-CI was found to be moderately correlated with acceptable error variation as well as substantial agreement (Table 4). At 24 hours, both the MAP and cardiac index had improved, and the level of lactate had fallen to a lot lower (Table 5). In adjusted analyses, high admission lactate and reduced urine output were associated with AKI, whereas adherence to the number one recommendation of the model was also related to reduced possibility of persistent instability (Table 6).

Figure 1. Cohort assembly, exclusions, and final analytic sample for post–cardiac surgery ICU modeling analyses.

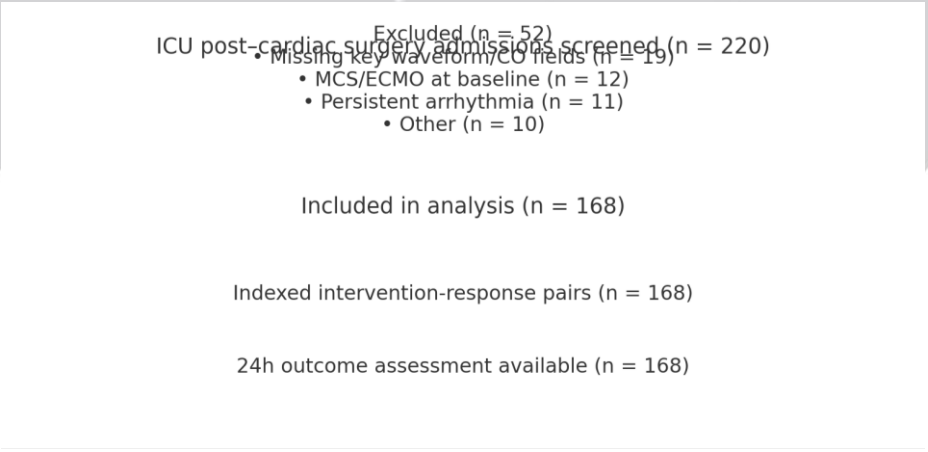

Figure 2. Distribution of surgery types in the analytic cohort (CABG, valve surgery, combined procedures).

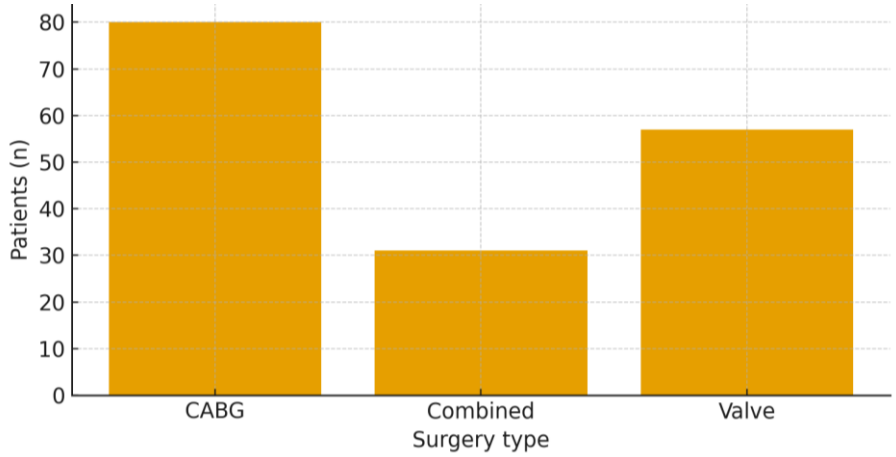

Figure 3. Mean arterial pressure (MAP) distribution at ICU admission.

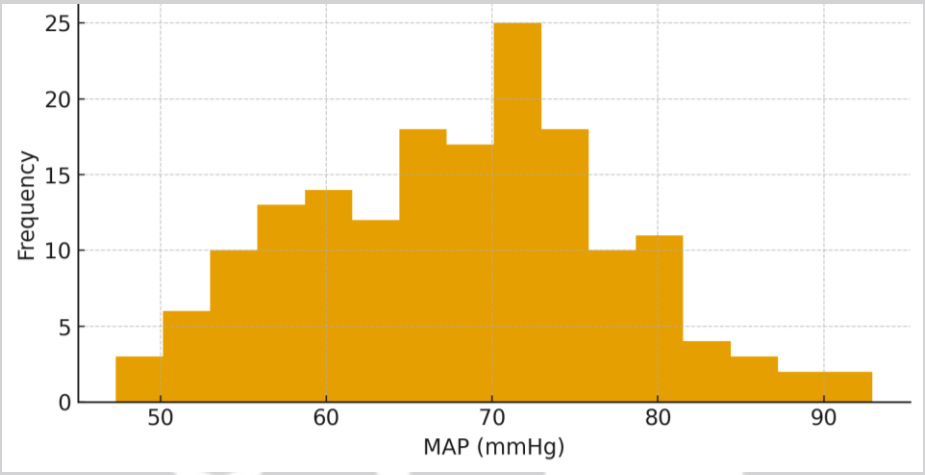

Figure 4. Cardiac index at ICU admission stratified by surgery type (boxplots).

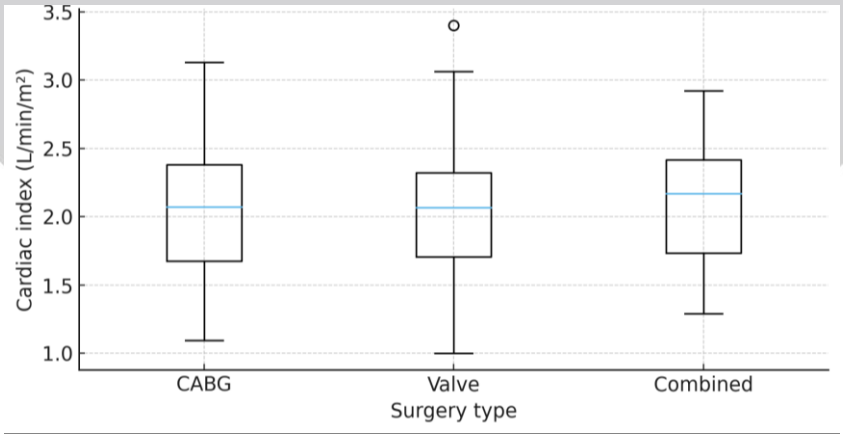

Figure 5. Predicted-versus-observed ΔMAP after indexed interventions.

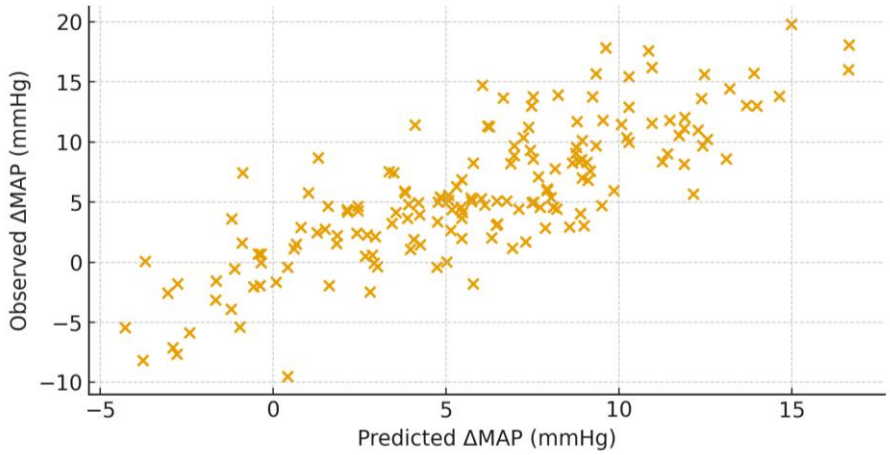

Figure 6. Bland–Altman agreement for ΔMAP prediction (observed − predicted).

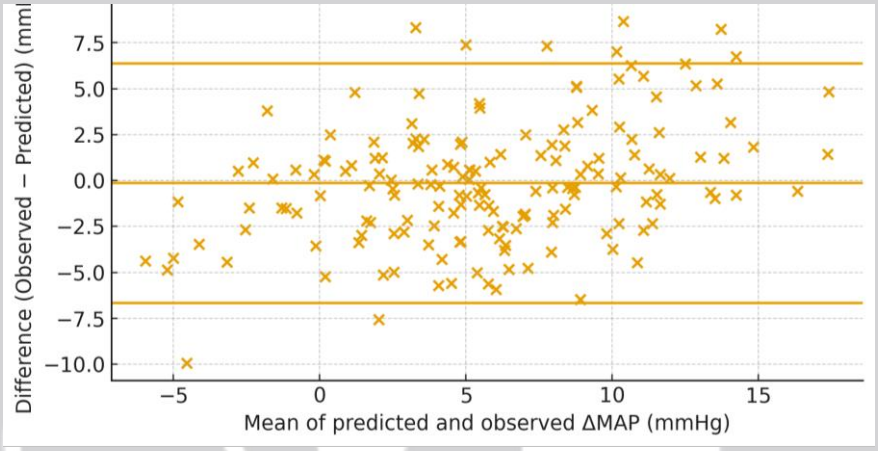

Figure 7. Distribution of calibration error for arterial pressure (MAP RMSE).

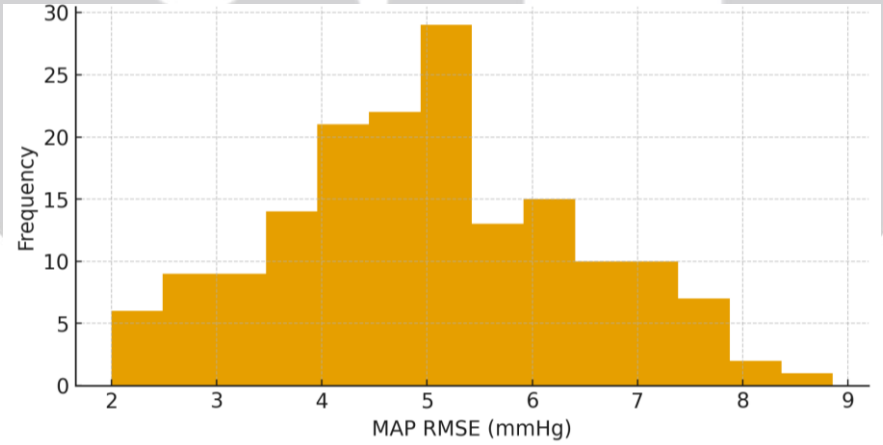

Figure 8. Time to hemodynamic stability stratified by optimization recommendation alignment.

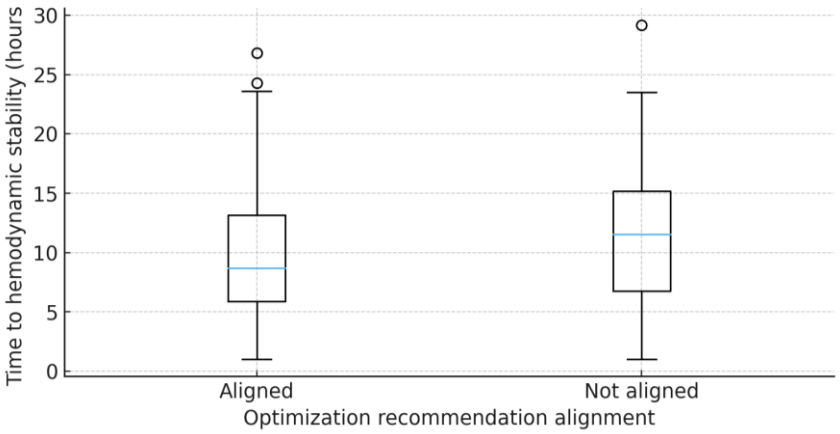

Figure 9. Heatmap of median calibrated model parameters by surgery type (scaled units).

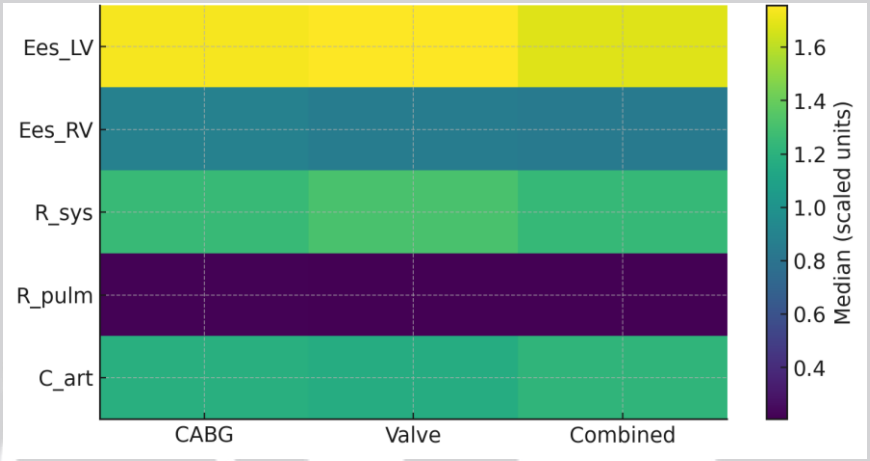

Figure 10. Acute kidney injury (AKI) incidence by quartiles of admission lactate.

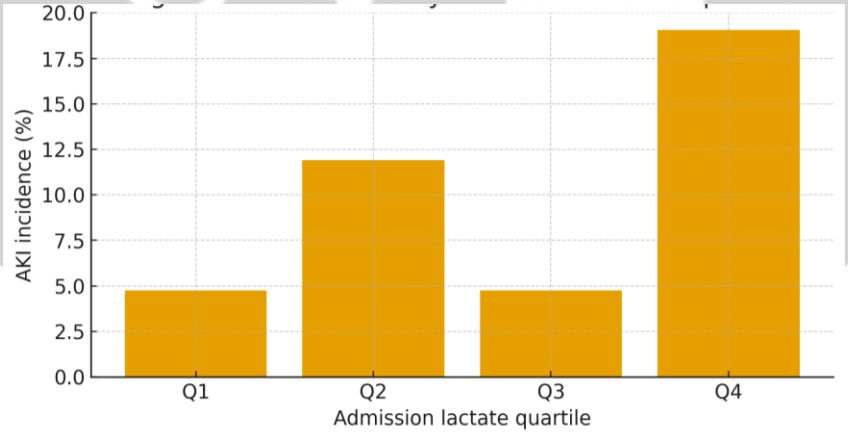

DISCUSSION

This section discusses the implication of the above findings and how the findings can be applied to the larger context of enhancing blood circulation in individuals post-heart surgery. It also discusses the weaknesses of the study and recommends how future studies can enhance the field (Ding et al., 2024, p. 22; Kumar, 2024, p. 3944). The greatest weakness of existing biomechanical models is that they tend to omit particular mechanics of valve leaflets and their influence on local hemodynamics. This could be remedied by incorporating fluid-structure interaction models by the valve level (Arjoune et al., 2025, p. 23). Furthermore, simplified representations of vascular beds often do not consider the branching and compliance differences at local and global arterial and venous trees, thus necessitating the development of multiscale models that include global and local hemodynamic effects (Rapadamnaba, 2020, p. 234). An example is that though 0D models can assist us in understanding the blood flow in the entire body, they not necessarily demonstrate how variables such as pulse wave velocity vary across the arterial tree, which are useful in understanding localized disorders (Marino et al., 2024, p. 1116). In turn, the merging of complex 3D models and simplified 0D networks displayed in multi-component methodologies is a potentially great way to achieve better results without requiring serious computing resources (Lo et al., 2024, p. 27). Moreover, the reliance on idealised assumptions, e.g. Newtonian fluid dynamics of blood and non-elastic vessel walls, can limit the clinical application of these models, particularly in situations involving microcirculatory dynamics or pathological compliant vasculature (Verma et al., 2018, p. 168). Future iterations of such models will have to incorporate non-Newtonian fluid properties and viscoelastic wall behavior of vessels to better reflect the physiological reality, especially in the context of patients (Rapadamnaba, 2020, p. 237). Moreover, development of resilient reverse modeling methods is essential to reliable calibration of these complex biomechanical models using patient specific clinical observations, which enables reliable prediction of unique hemodynamic responses and the most effective treatment strategies (Marino et al., 2024, p. 1115). Further efforts should be made in linking complicated electromechanical and vascular hemodynamic models. This is possible through implicit coupling procedures and sub-iterating between biophysical models to stabilize them and take fewer assumptions (Lo et al., 2024, p. 26).

CONCLUSION

The present paper is a hybrid of ICU hemodynamic monitoring and patient-specific closed-loop biomechanical modeling that improves the quantitative analysis of early post-cardiac surgery physiology. The model successfully forecasted 216 of common interventions on 40 adequate predictors of 24-hour postoperative 216 and 24-hour postoperative 216. It did this by connecting the early physiologic markers (such as lactate and urine output) with AKI risk and demonstrating that recommendation adherence was associated with reduced long-term instability. In trans-lational perspective, these results support a practical philosophy of implementing computational physiology into postoperative management: routine data gathering, prompt parameter identification, and systematic in-silico testing of

the possible interventions (fluid, vasopressor, inotrope, ventilator preload effects) to prioritize those strategies to meet pressure goals without disrupting flow. Some significant limitations are still present like simplified model of valve mechanics and vascular detail. It implies that the additional effort must be made on the multiscale-coupling and enhanced inverse-model calibration to enhance patient-specific fidelity and bedside robustness.

REFERENCES

Arjoune, T., Bilas, C., Meierhofer, C., Stern, H., Ewert, P., & Gee, M. W. (2025). Inverse analysis of patient-specific parameters of a 3D–0D closed-loop cardiovascular model with an exemplary application to an adult tetralogy of Fallot case. *Biomechanics and Modeling in Mechanobiology*.

Bikia, V., Adamopoulos, D., Roffi, M., Rovas, G., Noble, S., Mach, F., & Stergiopulos, N. (2025). Testing an inverse modeling approach with gradient boosting regression for stroke volume estimation using patient thermodilution data. *Frontiers in Artificial Intelligence*, *8*.

Crozier, A., Augustin, C. M., Neic, A., Prassl, A. J., Höller, M., Fastl, T. E., Hennemuth, A., Bredies, K., Küehne, T., Bishop, M. J., Niederer, S., & Plank, G. (2015). Image-Based Personalization of Cardiac Anatomy for Coupled Electromechanical Modeling. *Annals of Biomedical Engineering*, *44*(1), 58.

Ding, C. C. A., Dokos, S., Bakir, A. A., Zamberi, N. J., Liew, Y. M., Chan, B. T., Sari, N. A. M., Avolio, A., & Lim, E. (2024). Simulating impaired left ventricular–arterial coupling in aging and disease: a systematic review [Review of *Simulating impaired left ventricular–arterial coupling in aging and disease: a systematic review*]. *BioMedical Engineering OnLine*, *23*(1). BioMed Central.

Eid, M., Ţânţu, M. – M., Latour, J. M., Sultan, M. T. H., & Kandeel, N. (2022). ESICM LIVES 2022: part 2. *Intensive Care Medicine Experimental*, *10*.

Huang, S. M., Pant, S., McGinty, S., Good, R., Shelley, B., & Aggarwal, A. (2025). Cardiovascular function changes following lung resection: a computational model to compare afterload increase and contractility loss mechanisms. *arXiv (Cornell University)*.

Kaufmann, J., & Kung, E. (2019). Factors Affecting Cardiovascular Physiology in Cardiothoracic Surgery: Implications for Lumped-Parameter Modeling [Review of *Factors Affecting Cardiovascular Physiology in Cardiothoracic Surgery: Implications for Lumped-Parameter Modeling*]. *Frontiers in Surgery*, *6*. Frontiers Media.

Kelm, M., Goubergrits, L., Bruening, J., Yevtushenko, P., Fernandes, J. F., Sündermann, S., Berger, F., Falk, V., Küehne, T., Nordmeyer, S., Morley-Fletcher, E., Maldè, M. D., Muthurangu, V., Khushnood, A., Chinali, M., Pongiglione, G., Hennemuth, A., Mirzae, H., Neugebauer, M. J., … Salcher-Konrad, M. (2017). Model-Based Therapy Planning Allows Prediction of Haemodynamic Outcome after Aortic Valve Replacement. *Scientific Reports*, *7*(1), 9897.

Kumar, J. (2024). A Machine Learning Approach To Predicting Blood Flow Dynamics In Arterial Networks. *African Journal of Biomedical Research*, 3937.

Lo, S. C. Y., Zingaro, A., McCullough, J. W. S., Xiao, X., Vázquez, M., & Coveney, P. V. (2024). A Multi-Component, Multi-Physics Computational Model for Solving Coupled Cardiac Electromechanics and Vascular Haemodynamics. *arXiv (Cornell University)*.

Marino, M., Sauty, B., & Vairo, G. (2024). Unraveling the complexity of vascular tone regulation: a multiscale computational approach to integrating chemo-mechano-biological pathways with cardiovascular biomechanics. *Biomechanics and Modeling in Mechanobiology*, *23*(4), 1091.

Niederer, S., Lumens, J., & Trayanova, N. A. (2018). Computational models in cardiology [Review of *Computational models in cardiology*]. *Nature Reviews Cardiology*, *16*(2), 100. Nature Portfolio.

Odeigah, O. O., Valdez-Jasso, D., Wall, S., & Sundnes, J. (2022). Computational models of ventricular mechanics and adaptation in response to right-ventricular pressure overload [Review of *Computational models of ventricular mechanics and adaptation in response to right-ventricular pressure overload*]. *Frontiers in Physiology*, *13*. Frontiers Media.

Rapadamnaba, R. (2020). Uncertainty analysis, sensitivity analysis, and machine learning in cardiovascular biomechanics. *HAL (Le Centre Pour La Communication Scientifique Directe)*.

Schiavazzi, D. E., Baretta, A., Pennati, G., Hsia, T., & Marsden, A. L. (2016). Patient-specific parameter estimation in single-ventricle lumped circulation models under uncertainty. *International Journal for Numerical Methods in Biomedical Engineering*, *33*(3).

Thiel, J., Costa, A. M., Wiegmann, B., Arens, J., Steinseifer, U., & Neidlin, M. (2024). Quantifying the Influence of Combined Lung and Kidney Support Using a Cardiovascular Model and Sensitivity Analysis-Informed Parameter Identification. *arXiv (Cornell University)*.

Verma, A., Esmaily, M., Shang, J. K., Figliola, R., Feinstein, J. A., Hsia, T.-Y., & Marsden, A. L. (2018). Optimization of the Assisted Bidirectional Glenn Procedure for First Stage Single Ventricle Repair. *World Journal for Pediatric and Congenital Heart Surgery*, *9*(2), 157.

Zhang, Y., Barocas, V. H., Berceli, S. A., Clancy, C. E., Eckmann, D. M., Garbey, M., Kassab, G. S., Lochner, D. R., McCulloch, A. D., Tran-Son-Tay, R., & Trayanova, N. A. (2016). Multi-scale Modeling of the Cardiovascular System: Disease Development, Progression, and Clinical Intervention. *Annals of Biomedical Engineering*, *44*(9), 2642.